

Fluorine Abundances in Galactic AGB stars

C. Abia¹

Dpto. Física Teórica y del Cosmos, Universidad de Granada, 18071 Granada, Spain

`cabia@ugr.es`

K. Cunha²

National Optical Astronomy Observatory, P.O. Box 26732, Tucson, AZ 85726, USA

S. Cristallo¹

Dpto. Física Teórica y del Cosmos, Universidad de Granada, 18071 Granada, Spain

P. de Laverny³

University of Nice-Sophia Antipolis, CNRS (UMR 6202), Cassiopée, Observatoire de la Côte d'Azur, B.P. 4229, 06304 Nice Cedex 4, France

I. Domínguez¹

Dpto. Física Teórica y del Cosmos, Universidad de Granada, 18071 Granada, Spain

K. Eriksson⁴

Dept. of Physics & Astronomy, Uppsala University, Box 515, 751 20 Uppsala, Sweden

L. Gialanella⁵

INFN Sezione di Napoli, Naples, Italy

K. Hinkle⁶

National Optical Astronomy Observatory, P.O. Box 26732, Tucson, AZ 85726, USA

G. Imbriani⁵

Dipt. di Scienze Fisiche, Università Federico II, Naples, Italy

A. Recio-Blanco³

University of Nice-Sophia Antipolis, CNRS (UMR 6202), Cassiopée, Observatoire de la Côte d'Azur, B.P. 4229, 06304 Nice Cedex 4, France

V.V. Smith⁶

National Optical Astronomy Observatory, P.O. Box 26732, Tucson, AZ 85726, USA

O. Straniero⁷

INAF-Osservatorio di Collurania, 64100 Teramo, Italy

and

R. Wahlin⁴

Dept. of Physics & Astronomy, Uppsala University, Box 515, 751 20 Uppsala, Sweden

ABSTRACT

An analysis of the fluorine abundance in Galactic AGB carbon stars (**24 N-type, 5 SC-type and 5 J-type**) is presented. This study uses the state-of-the-art carbon rich atmosphere models and improved atomic and molecular line lists in the 2.3 μm region. F abundances significantly lower are obtained in comparison to previous study in the literature. The main reason of this difference is due to molecular blends. In the case of carbon stars of SC-type, differences in the model atmospheres are also relevant. The new F enhancements are now in agreement with the most recent theoretical nucleosynthesis models in low-mass AGB stars, solving the long standing problem of F in Galactic AGB stars. Nevertheless, some SC-type carbon stars still show larger F abundances than predicted by stellar models. The possibility that these stars are of larger mass is briefly discussed.

Subject headings: stars: abundances — stars: carbon — stars: AGB and post-AGB — nuclear reactions, nucleosynthesis, abundances

1. Introduction

The first observational evidence of ^{19}F stellar nucleosynthesis was reported by Jorissen, Smith & Lambert (1992, hereafter JSL). These authors derived F enhancements up to a factor 50 solar in a sample of Galactic AGB stars, and found a correlation between this enhancement and the C/O ratio. Since the C/O is expected to increase as a consequence of third dredge up (TDU) episodes during the AGB phase (e.g. Busso et al. 1999), this

was interpreted as a clear evidence of F production in these stars. Further observational evidence of such a production exists from studies of post-AGB stars (Werner, Rauch & Kruk 2005) and planetary nebulae (Otsuka et al. 2008). Other sites for F production have also been proposed: Wolf-Rayet stars (Meynet & Arnould 2000) and neutrino spallation in core-collapse supernovae (Woosley & Haxton 1988). However, the role of these sources in the F budget is still uncertain (Cunha et al. 2003; Palacios, Arnould & Meynet 2005). Nevertheless, from Galactic chemical evolution models, Renda et al. (2004) concluded that all three of these three sources are required to explain the observed Galactic evolution of F, as deduced from abundance determinations in field stars (Cunha & Smith 2005; Cunha, Smith & Gibson 2008), although, only in AGB stars there exist an observational confirmation that F production is an ongoing process.

Fluorine can be produced in AGB stars from the nuclear chain $^{14}\text{N}(\alpha, \gamma)^{18}\text{F}(\beta^+)^{18}\text{O}(p, \alpha)^{15}\text{N}(\alpha, \gamma)^{19}\text{F}$; where protons are mainly provided by $^{14}\text{N}(n, p)^{14}\text{C}$ and neutrons by $^{13}\text{C}(\alpha, n)^{16}\text{O}$. However, the theoretical attempts made to explain the JSL results are unsatisfactory. The problem is that current AGB models fail to explain the highest F enhancements found in the C-rich objects of the JSL sample (Goriely & Mowlavi 2000; Lugaro et al. 2004). This discrepancy has led to a deep revision of the uncertainties in the nuclear reaction rates involved in the synthesis of F in AGB stars (Lugaro et al. 2004; Stancliffe et al. 2005), to argue for alternative nuclear chains and/or to propose the existence of non-standard mixing/burning processes, similar to those commonly used to explain some of the isotopic anomalies found in dust grains formed in the envelopes of AGB stars (e.g. Nollett et al. 2003; Busso et al. 2007). However, no solution has been found up to date, leaving the subject of the origin of this element open.

Very recently, Abia et al. (2009, hereafter Paper I) derived F abundances from VLT spectra in three Galactic AGB C-stars in common with the JSL sample, namely: AQ Sgr, TX Psc (N-type) and R Scl (J-type), by using mainly the HF R9 line at $\lambda 2.3358 \mu\text{m}$. In that work, we showed that this HF line is almost free of blends in AGB C-stars and thus is probably the best tool for F abundance determinations in these stars (see also Uttenthaler et al. 2008). For these three stars, we derived F abundances ~ 0.7 dex lower in average than those obtained by JSL. We ascribed this difference to molecular blends (mainly of C_2 and CN). These new F abundances are in better agreement with the most recent theoretical nucleosynthesis predictions in low-mass ($< 3 M_{\odot}$) TP-AGB models (Cristallo et al. 2009). Motivated by this result, we have reanalysed the F abundances in the whole C-stars sample studied by JSL using the same tools as in Paper I. In this Letter, we confirm the results found in Paper I and show that the new F abundances nicely agree with the theoretical predictions of low-mass TP-AGB models. This apparently solves the long standing problem of F enhancements in AGB stars without requiring the existence of any extra mixing/burning

process.

2. Analysis and Results

Our data consist of high-resolution spectra **from** ~ 1.5 to **2.5** μm obtained with the 4 m telescope at Kitt Peak Observatory and a Fourier Transform Spectrometer, which have been used in several abundance analysis of AGB stars (see Lambert et al. 1986 and JSL for details). Typical resolutions ranged from 0.05 to 0.14 cm^{-1} ($R= 87000$ to 30000). These spectra contain many HF lines of the vibrational 1-0 band although we used only the lines R9 to R23. High resolution optical spectra ($R\sim 160000$) **in the range** $\lambda 4600 - 8000 \text{ \AA}$ obtained at the 3.5 m TNG at La Palma Observatory with SARG echelle spectrograph were also analysed. These spectra served us to derive the *s*-element content in **the stars BL Ori, ST Cam, Y Tau, CY Cyg, RZ Peg and GP Ori using the same procedure as in Abia et al. (2002)**. All program stars were ratioed with hot stars to remove telluric spectral features by using the task *telluric* within the IRAF package. The typical S/N ratio of the spectra is larger than 100. We adopted the stellar parameters (T_{eff} , $\log g$, $[\text{Fe}/\text{H}]$, ξ , **CNO abundances**, C/O and $^{12}\text{C}/^{13}\text{C}$ ratios) derived by previous studies: Abia et al. (2002) and Lambert et al. (1986) for N-type stars, Abia & Isern (2000) for J-type stars and Zamora (2009) for stars of SC-type (see these works for details). In addition, we also adopted the $^{16}\text{O}/^{17}\text{O}/^{18}\text{O}$ ratios from the literature when available (Harris et al. 1987), although this has a minimal impact on the derived F abundance. The method of analysis involves the comparison of theoretical LTE spectra (computed with the *Turbospectrum* code) with the observed ones. We used the latest generation of C-rich atmosphere models for giant stars (Gustafsson et al. 2008) and up-to-date molecular and atomic line lists in the spectral ranges studied (see Paper I for details).

Figure 1 shows an example of comparison between the observed and theoretical spectrum for the C-star UU Aur (N-type) in two different spectral ranges. In particular, top panel shows the fit to the R15 and R16 HF lines, the sole lines used by JSL to derive the F abundance in the C-rich objects. It can be seen that we can reproduce reasonably well the observed spectrum and that the synthetic spectrum computed with the F abundance obtained by JSL (lower dashed line), would overestimate the F abundance in this star. Our best estimation in this star ($\log \epsilon(F) = 4.88$, continuous line in Fig. 1) fits quite well the six HF lines used, with a dispersion of only ± 0.04 dex (see also Table 1)¹. Similar quality

¹We notice, that the F abundances derived in the stars AQ Sgr and R Scl by using both CRIRES and FTS spectra are in perfect agreement.

fits were obtained for all the stars except for V Hya, which was excluded from the analysis since its effective temperature is outside the range covered by our grid of models. Table 1 lists the final F abundance derived in each star, assigning double weight to the R9 line when estimating the mean F abundance because this is the less blended among the available HF lines (see Paper I for a discussion). For most of the stars, more than three different HF lines were used. The agreement between the different lines is in general good with a typical mean dispersion of ± 0.08 dex. The formal error in the F abundance due to uncertainties in the stellar parameters ranges from 0.20 – 0.30 dex, depending on the particular HF line. Considering the abundance dispersion and the uncertainty in the continuum position as additional sources of error, we estimate an total uncertainty of $\pm 0.30 - 0.35$ dex in the $[F/H]^2$ ratio (see Paper I). However, the abundance ratio between F and any other element typically has a smaller error since some of the above uncertainties cancel out when deriving the abundance ratio: for the $[F/Fe]$ ratio we estimate a total uncertainty of ± 0.25 dex.

The third column in Table 1 shows the difference found between the F abundance derived by JSL and this work. The differences range from 0.3 dex up to more than 1 dex, the average value being $\Delta \log \epsilon(F) = +0.7$, confirming the main result of Paper I. As noted there, differences in the stellar parameters adopted in the analysis cannot explain this discrepancy. Actually, the major differences are found for the T_{eff} values, which for the N- and J-type stars in the sample, do not exceed 150 K. In the case of SC-type stars, differences in adopted T_{eff} may reach up to 300 K, but in any case, this cannot explain the differences of more than ~ 1 dex in the F abundance found in some of these stars. Differences in the atomic data are also discarded since we used exactly the same HF line list than JSL. Finally, differences between the grid of model atmospheres might account up to a maximum of 0.15 dex, for the N- and J-type stars. For the SC-type stars, we found the largest abundance differences (see Table 1). For these stars, atmosphere models indeed play a significant role. JSL used for the analysis of SC stars Johnson (1982) models, while we use those from Gustafsson et al. (2008). **For instance, considering the typical stellar parameters of a SC star in the sample ($T_{eff}/\log g/[Fe/H] = 3500/0.0/0.0$ and $C/O = 1.0$), we find differences in the F abundance from +0.4 dex (R9, R15 and R16 lines) to +0.02 dex (R23 line) when using Johnson models instead of Gustafsson et al. ones, but it may reach up to +0.6 dex for lower T_{eff} .** In any case, for the N- and J-type stars, we conclude (as in Paper I) that the difference between the molecular line list used is the main cause of the discrepancy with respect to the analysis of JSL (see Table 2). For the SC-type stars, it is a combination of that, the use of a different grid of model atmospheres and, in the case of CY Cyg and GP Ori, the adoption here of a $T_{eff} \sim 300$ K cooler. It should be mentioned that the structure

²The solar F abundance adopted here is 4.56 (Grevesse, Asplund & Sauval 2007).

of the C-rich atmosphere models change dramatically with a tiny variation of the C/O ratio when it is very close to 1, as it is the case for SC stars. Therefore, the abundance analysis in these stars are affected by systematic differences between the model atmosphere and the real star and/or the treatment of the molecular equilibrium in the computation of the atmosphere models. In consequence, for SC-type stars the uncertainty in [F/H] is certainly larger than ± 0.3 dex.

3. Discussion

The main consequence of the new F abundances is that the large [F/Fe] (or [F/O]) ratios (up to 1.8 dex) found by JSL in Galactic AGB C-stars are systematically reduced. The largest F enhancements are now close to ~ 1 dex. These enhancements can be accounted for by current low-mass TP-AGB nucleosynthesis models of solar metallicity, as we will show below. As noted in §1, during the ascension along the AGB, fresh carbon is mixed within the envelope due to TDU episodes. Eventually, an O-rich AGB star becomes a C-star when the C/O ratio in the envelope exceeds 1. Similarly, F is also expected to increase in the envelope during the AGB phase, thus a fluorine vs. carbon correlation should exist. Figure 2 shows the observed relationship derived in this study. We have also included in this figure the intrinsic³ O-rich AGB stars studied by JSL (not analysed here, open circles). Excluding the J-type⁴ stars (triangles), a clear increase of the F abundance with the C abundance can be seen. This behaviour is well reproduced by theoretical AGB models. Lines in Fig. 2 show the predicted F and C content in the envelope (Cristallo et al. 2010) for a $1.5 M_{\odot}$ with different metallicities (continuous lines) and $2 M_{\odot}$ model (dashed line) with solar metallicity. These metallicities match those of the stellar sample ($-0.5 \leq [\text{Fe}/\text{H}] \leq 0.1$). The theoretical curves start with an envelope composition as determined by the first dredge-up and end at the last TDU episode. On the other hand, Fig. 2 seems to indicate that O-rich stars and SC stars (squares) have F abundances systematically larger than N-type stars (dots) for a given C abundance. Similarly to the intrinsic C-stars, also in the case of the O-rich stars

³Intrinsic AGB stars have their envelopes polluted by nucleosynthesis products made *in situ*. Extrinsic stars, on the contrary, own their chemical peculiarities to a mass transfer episode in a binary system. All the O-rich stars shown in Fig. 2 show ^{99}Tc ($\tau_{1/2} \sim 2 \times 10^5$ yr) in their envelopes (Smith & Lambert 1990), revealing their intrinsic nature.

⁴The origin of J-type C-stars is still unknown. They are slightly less luminous than N-type C-stars and show chemical peculiarities rather different with respect to these stars (e.g. Abia & Isern 2000). It has been suggested that they might be the descendants of the early R-type stars, however this has been questioned recently (Zamora 2009).

this may be simply due to a systematic error affecting the analysis: in fact, for stars of spectral types K and M (with $[\text{Fe}/\text{H}] \sim 0.0$), JSL derived an average F abundance ~ 0.13 dex higher (4.69) than the solar F abundance adopted here (4.56). These K and M stars are sub-giants or RGB stars, thus they are not expected to present F enhancements. Excluding that the Sun might be anomalous with respect to nearby stars of similar metallicity (F determinations in unevolved dwarf stars are needed in this sense), blends may also play a role in the analysis of F lines in O-rich AGB stars. Decreasing the F abundances by 0.13 dex in them, the agreement with theoretical predictions would be definitely better. However, it does not apply to the case of the star BD+48°1187 (at $\log \epsilon(\text{F}) \sim 5.5$ in Fig. 2); the large F enhancement in this star can be only obtained in metal-poor AGB models, but this star has $[\text{Fe}/\text{H}] = 0.07$. Something similar seems to occur with SC-type stars. SC stars are AGB stars with $\text{C}/\text{O} \approx 1$. According to the accepted chemical (spectral) evolution along the AGB ($\text{M} \rightarrow \text{MS} \rightarrow \text{S} \rightarrow \text{SC} \rightarrow \text{N}$), these stars should present equal-or-slightly lower F enhancements than N-type stars. However, some of the studied SC stars clearly deviate from this sequence, showing larger F abundances with respect to N stars. This is reinforced by WZ Cas⁵ ($[\text{Fe}/\text{H}] \sim 0.0$, at the right upper corner of Fig. 2), which shows a huge F enhancement. We remind, however, that this star is indeed peculiar: it is one of the few super Li-rich C-stars known, also presenting very low $^{12}\text{C}/^{13}\text{C}$ (4.5) and $^{16}\text{O}/^{17}\text{O}$ (400) ratios. The fact that most of the SC-stars studied here show low or no s -element enhancements (see below), makes the evolutionary status of these stars very uncertain.

The connection between the F and the s -process is less straightforward. There are two different contributions to the F production in low mass AGB stars. The first comes from the ^{15}N production in the radiative ^{13}C pocket, the site where the s -process main component is built up: when, during the interpulse period, the $^{13}\text{C}(\alpha, n)^{16}\text{O}$ is activated within the pocket, some protons are released by the main poisoning reaction, $^{14}\text{N}(n, p)^{14}\text{C}$, thus producing ^{15}N via $^{18}\text{O}(p, \alpha)^{15}\text{N}$. The second contribution involves the same reaction chain, but it is activated when the ^{13}C left by the advancing H-burning shell is engulfed into the convective zone generated by a thermal pulse. In the latter case, the correlation with the s -process is less stringent, because the resulting neutron flux is not enough to give rise to a sizable production of elements beyond iron. At nearly solar metallicity, the latter contribution accounts for $\sim 70\%$ of the total F production (e.g. **Cristallo 2006**). Nevertheless, a correlation between the F and the s -element overabundance is in any case expected if a large enough ^{13}C pocket forms after each dredge up episode. Figure 3 shows the new $[\text{F}/\text{Fe}]$ ratios in C-stars vs. the observed average s -element enhancement (**from Abia et al. 2002; Zamora 2009 or derived in this work, see §1**). J-type stars are not

⁵This star has also been classified as J-type.

shown in this figure as they do not have s -element enhancements (see Table 1; Abia & Isern 2000). Similarly to Fig. 2, we have included the intrinsic O-rich stars analysed by JSL taken their s -element content from Smith & Lambert (1990). It is clear that the F and s -nuclei overabundances correlate and that this correlation is nicely reproduced by theoretical TP-AGB stellar models (Cristallo et al. 2010). The theoretical predictions in Fig. 3 correspond to 1.5, 2 and 3 M_{\odot} TP-AGB models with $Z=0.008$ ($[Fe/H]\sim -0.25$, the average metallicity of the stars analysed here) starting from the 1st TP pulse. The number of TPs calculated until the occurrence of the last TDU is indicated in the figure for each model. Models with a metallicity within $\sim \pm 0.2$ dex of this value do not significantly differ from those in Figure 3. In addition, with the combination of models with different stellar mass and metallicity, it is possible not only to reproduce the new observed $[F/Fe]$ vs. s -element relationship, but also the detailed F and s -element abundance pattern observed in a particular star (see e.g. Fig. 3 in Paper I). Note that this is not possible for most of the stars when adopting the F determinations of JSL.

As already noted, SC-type stars (except GP Ori) show larger F abundances than predicted by low-mass AGB models with the same s -element enhancement. A possible explanation could be that the SC stars are more massive (in average) than the bulk of the N-type C-stars. From AGB models with mass of about 3-5 M_{\odot} , we expect smaller ^{13}C pockets and weaker s -element surface enrichments, even if the number of TPs and TDU episodes is larger. It occurs because the larger the core mass is, the smaller the He-rich intershell is with a steeper pressure gradient. Notwithstanding, the ^{13}C left in the ashes of the H-shell still provide a substantial contribution to the fluorine production. Recent studies of the luminosity function of Galactic C-stars (Guandalini 2008) support such a hypothesis. They indicate that the SC-type stars are among the most luminous AGB C-stars. Once again, the case of WZ Cas is particularly extreme. This star shows a huge F abundance ($[F/Fe]= +1.15$) with almost no s -element enhancement. Its large Li abundance might be interpreted as a consequence of the hot bottom burning (HBB) mechanism which operates only for $M \geq 5 M_{\odot}$. **However, the operation of the HBB would be at odds with the presence of F in the envelope since $^{19}F(p, \alpha)^{16}O$ might destroy ^{19}F .** Detailed abundance studies (including F) in a larger sample of SC-stars is needed to confirm this hypothesis.

4. Summary

Fluorine abundances in Galactic AGB carbon stars are determined from high resolution infrared spectra using state-of-the-art C-rich spherical model atmospheres, updated atomic and molecular line lists and LTE spectral synthesis. We derive F abundances that are

in average ~ 0.7 dex lower than those derived in previous studies. A clear correlation between the F and s–element enhancements is found. The new fluorine enhancements can be explained by standard low-mass AGB stellar models. F abundance determinations appear as a valuable tool to test theoretical AGB models. Studies of the F abundance in metal poor unevolved and AGB stars are mandatory to understand the Galactic abundance evolution of this element and to evaluate the role of AGB stars in its origin, respectively.

Part of this work was supported by the Spanish grants AYA2008-04211-C02-02 and FPA2008-03908 from the MEC. P. de Laverny and A. Recio-Blanco acknowledge the financial support of Programme National de Physique Stellaire (PNPS) of CNRS/INSU, France. KE gratefully acknowledges support from the Swedish Research Council. We are thankful to B. Plez for providing us molecular line lists in the observed infrared domain.

Facilities: ORM TNG (SARG) and NOAO Kitt peak (FTS).

REFERENCES

- Abia, C., & Isern, J. 2000, ApJ, 536, 438
- Abia, C., et al. 2002, ApJ, 578, 817
- Abia, C., et al. 2009, ApJ, 694, 971 (Paper I)
- Busso, M., Gallino, R., & Wasserburg, G.J. 1999, ARA&A, 37, 239
- Busso, M., Wasserburg, G.J., Nollett, K.M., & Calandra, A. 2007, ApJ, 671, 802
- Cristallo, S. 2006, PASP, 118, 1360
- Cristallo, S., et al. 2009, ApJ, 696, 797
- Cristallo, S. et al. 2010, in preparation
- Cunha, K., Smith, V.V., Lambert, D.L., & Hinkle, K.H. 2003, AJ, 126, 1305
- Cunha, K., & Smith, V.V. 2005, ApJ, 626, 425
- Cunha, K., Smith, V.V., & Gibson, B. 2008, ApJ, 679, L17
- Goriely, S., & Mowlavi, N. 2000, A&A, 362, 599
- Grevesse, N., Asplund, M., & Sauval, A.J. 2007, Space Science Reviews, 130, 105

- Guandalini, R. 2008, AIP Conf. Proc., 1001, 339
- Gustafsson, B. et al. 2008, A&A, 486, 951
- Harris, M.J., et al. 1987, ApJ, 316, 294
- Johnson, H.R. 1982, ApJ, 260, 254
- Jorissen, A., Smith, V.V., & Lambert, D.L. 1992, A&A, 261, 164 (JSL)
- Lambert, D.L., Gustafsson, B., Eriksson, K, Hinkle, K.H. 1986, ApJS, 62, 373
- Lugaro, M. et al. 2004, ApJ, 615, 934
- Meynet, G., & Arnould, M. 2000, A&A, 335, 176
- Nollett, K.M., Busso, M., & Wasserburg, G.J. 2003, ApJ, 582, 1036
- Otsuka, M., Izumiura, H., Tajitsu, A., & Hyung, S. 2008, ApJ, 682, L108
- Palacios, A., Arnould, M., & Meynet, G. 2005, A&A, 443, 243
- Renda, A., et al. 2004, MNRAS, 354, 575
- Smith, V.V., & Lambert, D.L. 1990, ApJS, 72, 387
- Stancliffe, R.J., et al. 2005, MNRAS, 360, 375
- Uttenthaler, S. et al. 2008, ApJ, 682, 509
- Werner, K., Rauch, T., & Kruk, J.W. 2005, A&A, 433, 641
- Woosley, S.E., & Haxton, W.C. 1988, Nature, 334, 5
- Zamora, O. 2009, Ph. D. Thesis, University of Granada

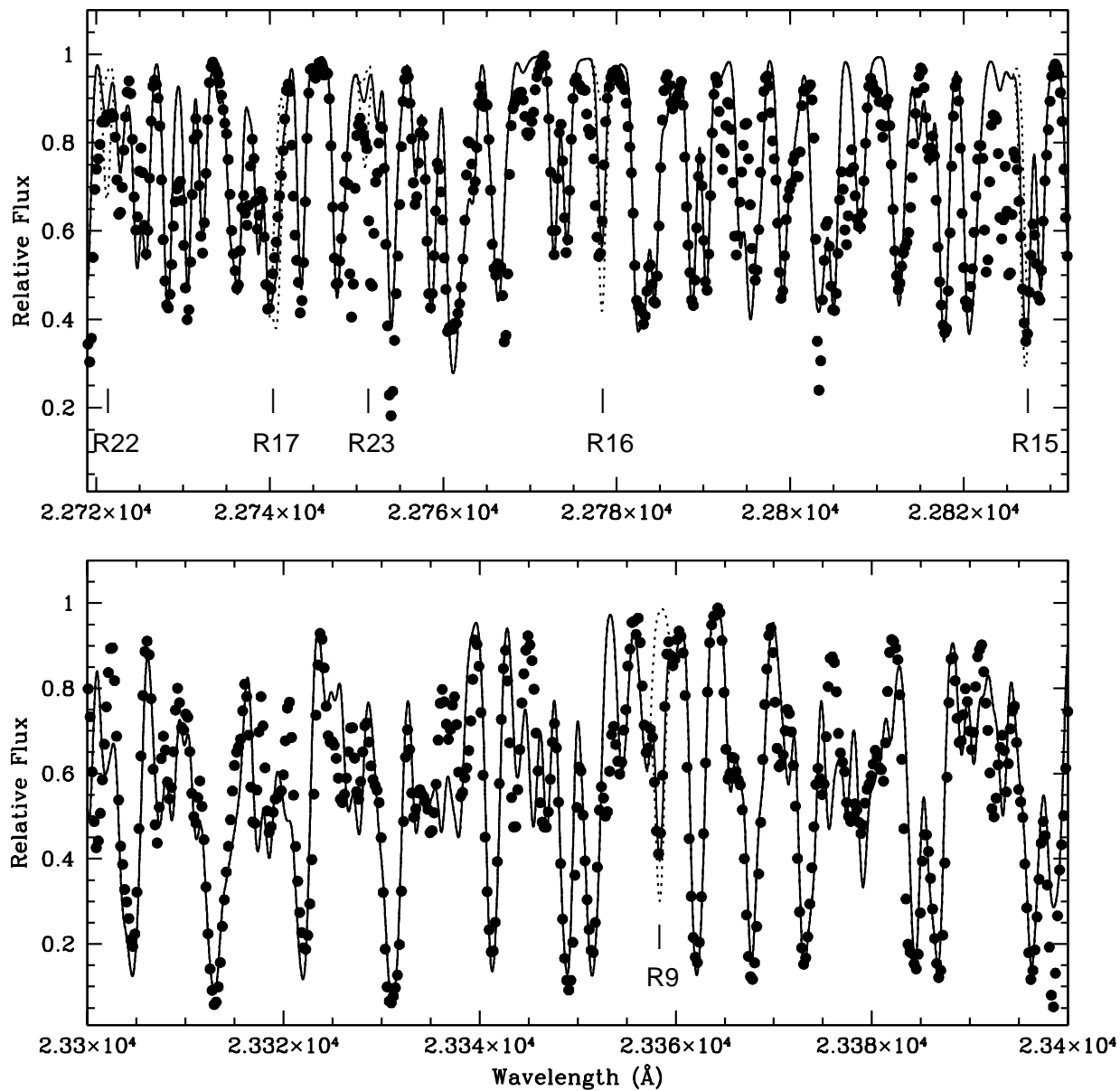


Fig. 1.— Comparison of the observed and synthetic spectrum of UU Aur (dots) with an identification of the available HF lines. Dashed lines represent the synthetic spectra calculated with no F and with the abundance value obtained by JSL, respectively. The continuous line is the synthetic spectrum calculated with the abundance given in Table 1, $\log \epsilon(\text{F}) = 4.88$.

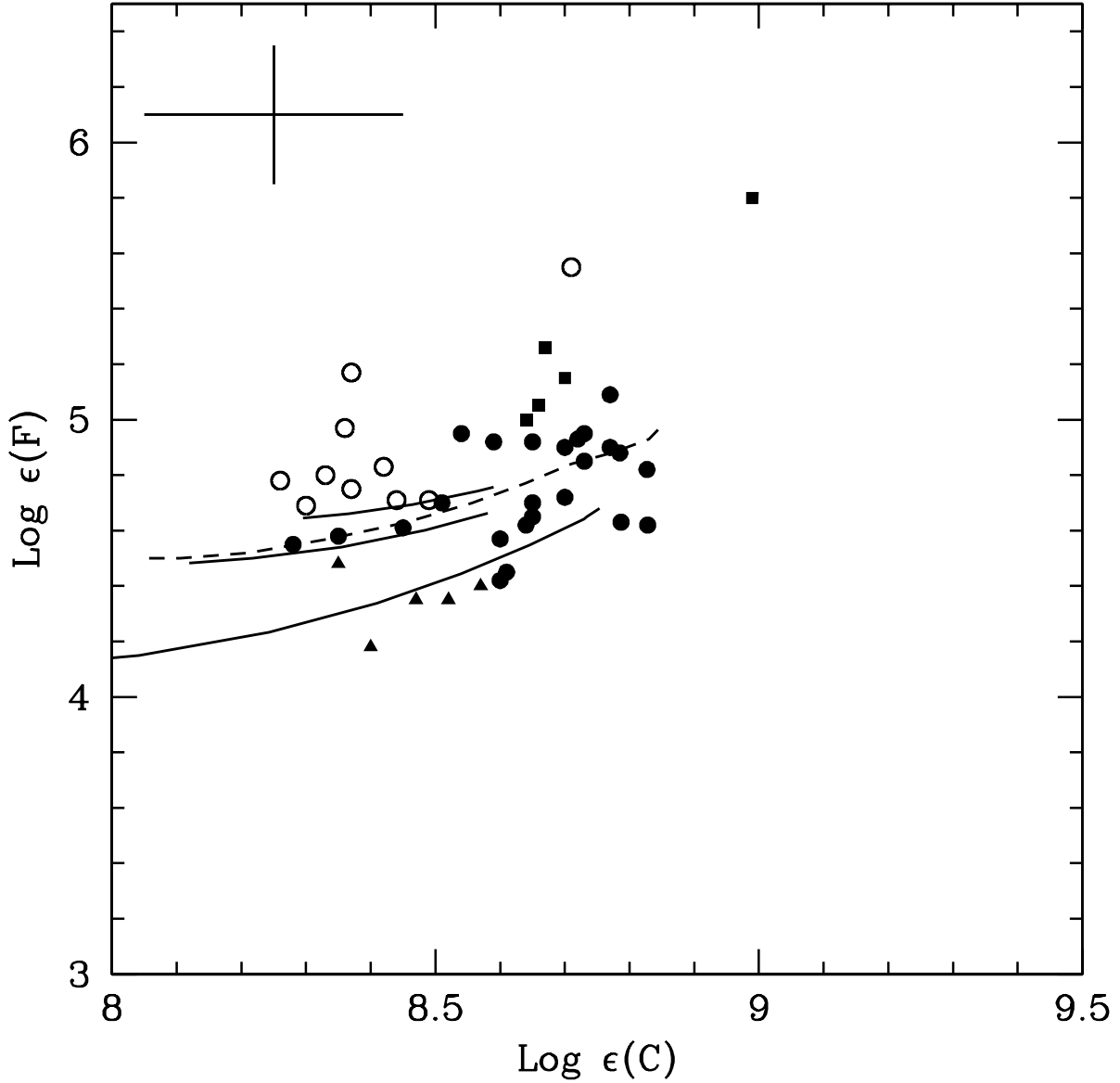


Fig. 2.— Logarithmic abundances of fluorine vs. carbon. Symbols: filled circles, N-stars; triangles, J-type; squares, SC-type; open circles, intrinsic O-rich AGB stars from JSL. Lines are theoretical predictions for a $1.5 M_{\odot}$, TP-AGB model with metallicities $Z = 0.02$, Z_{\odot} and 0.006 (continuous lines from up to down), and a $2 M_{\odot}$, $Z = Z_{\odot}$ model (dashed line), respectively.

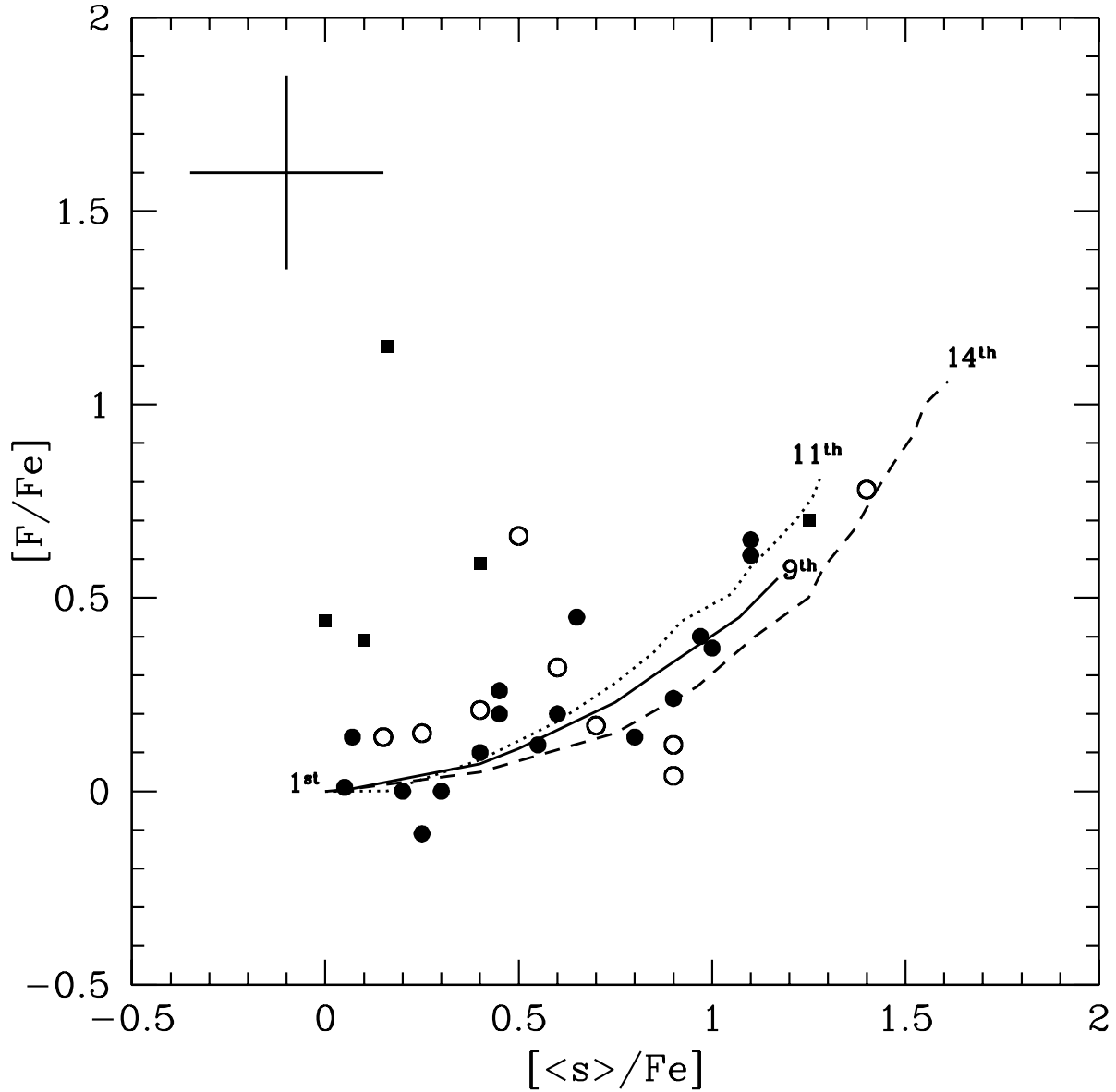


Fig. 3.— Fluorine vs. average s-element enhancements in galactic AGB stars. Symbols as in Fig 2. Lines are theoretical predictions for 1.5, 2 and 3 M_{\odot} , $Z = 0.008$ TP-AGB models (solid, dashed and dotted lines, respectively) from Cristallo et al. (2010). The number of TPs achieved by each models is also indicated.

Table 1. Abundances.

Star	$\log \epsilon(\text{F})^{\text{a}}$	$\Delta \log \epsilon(\text{F})^{\text{b}}$	C/O	[F/Fe]	[<s>/Fe]
<i>N stars</i>					
AQ Sgr	4.63±0.02 (4)	0.85	1.03	0.10	...
BL Ori	4.92±0.17 (4)	0.57	1.04	0.37	1.00
R Lep	4.45±0.20 (2)	0.47	1.03	0.34	...
RT Cap	4.95±0.01 (5)	0.36	1.10	0.40	...
RV Cyg	4.70±0.10 (4)	0.63	1.20	0.15	0.07
S Sct	4.62±0.03 (4)	1.08	1.07	0.10	0.40
SS Vir	4.55±0.07 (2)	...	1.05	0.00	0.30
ST Cam	4.72±0.14 (4)	0.94	1.14	0.20	0.45
TU Gem	4.92±0.07 (5)	0.88	1.12	0.36	...
TW Oph	4.61±0.06 (3)	0.30	1.20	0.46	...
TX Psc	4.82±0.10 (6)	0.73	1.03	0.65	1.10
U Cam	4.58±0.07 (4)	0.54	1.30	0.12	0.55
U Hya	5.09±0.08 (5)	...	1.05	0.61	1.10
UU Aur	4.88±0.04 (5)	0.76	1.06	0.26	0.45
UX Dra	4.85±0.15 (4)	0.64	1.05	0.45	0.65
V460 Cyg	4.65±0.10 (4)	0.68	1.06	0.14	0.80
V Aql	4.62±0.14 (5)	0.54	1.25	0.00	0.20
VY UMa	4.70±0.08 (3)	1.02	1.06	0.24	0.90
W CMa	4.95±0.08 (6)	0.56	1.05	0.20	0.60
W Ori	4.42±0.05 (4)	0.65	1.16	-0.11	0.25
X Cnc	4.93±0.10 (3)	0.76	1.14	0.67	...
Y Hya	4.90±0.02 (5)	0.33	1.52	0.44	...
Y Tau	4.57±0.09 (6)	0.49	1.04	0.01	0.05
Z Psc	4.90±0.13 (4)	0.42	1.01	0.40	0.97
<i>SC stars</i>					
CY Cyg	5.05±0.05 (4)	0.98	1.04	0.39	0.10
FU Mon	5.15±0.10 (5)	1.35	1.00	0.59	0.40
GP Ori	5.26±0.08 (6)	0.94	1.00	0.70	1.25
RZ Peg	5.00±0.10 (6)	1.06	1.00	0.44	0.00

Table 1—Continued

Star	$\log \epsilon(\text{F})^{\text{a}}$	$\Delta \log \epsilon(\text{F})^{\text{b}}$	C/O	[F/Fe]	[<s>/Fe]
WZ Cas	5.80 ± 0.17 (6)	0.40	1.01	1.15	0.16
<i>J stars</i>					
R Scl	4.18 ± 0.03 (3)	1.22	1.34	0.09	...
RY Dra	4.48 ± 0.06 (3)	0.44	1.18	-0.08	<0.20
T Lyr	4.35 ± 0.00 (2)	0.45	1.29	-0.21	...
VX And	4.35 (1)	...	1.76	-0.20	0.2
Y Cvn	4.40 (1)	0.50	1.09	-0.10	<0.2

Note. — The abundances of fluorine are given using the definition $\log \epsilon(\text{X}) = 12 + \log (\text{X}/\text{H})$, where (X/H) is the abundance of the element X by number.

^aThe number in parenthesis indicates the number of HF lines used.

^bAbundance difference with respect to JSL.

Table 2. Main blends affecting the HF lines.

HF line	Blend	$\Delta[\text{C}/\text{H}] = \pm 0.2^{\text{a}}$
R9	...	∓ 0.01
R15	$^{12}\text{C}^{14}\text{N}$, λ 22827.354	∓ 0.25
R16	$^{12}\text{C}^{12}\text{C}$, λ 22778.775	∓ 0.15
R17	$^{12}\text{C}^{14}\text{N}$, λ 22740.700	∓ 0.03
R22	$^{13}\text{C}^{14}\text{N}$, λ 22721.294	∓ 0.05
R23	$^{12}\text{C}^{14}\text{N}$, λ 22751.140	∓ 0.02

^aVariation of the F abundance derived from each HF line due to changes in the carbon abundance for a representative case $T_{eff}/\log g/[\text{Fe}/\text{H}] = 2800/0.0/0.0$ and $\text{C}/\text{O} = 1.06$.